Manipulation of polarization-dependent multivortices with quasi-periodic subwavelength structures

Gabriel Biener, Yuri Gorodetski, Avi Niv, Vladimir Kleiner, and Erez Hasman

Optical Engineering Laboratory, Faculty of Mechanical Engineering, Technion-Israel Institute of Technology, Haifa 32000, Israel

Received February 15, 2006; revised March 21, 2006; accepted March 24, 2006; posted March 27, 2006 (Doc. ID 68118)

Multiple vortices with different topological charges are formed by the use of two sequential geometric phase elements. These elements are realized by quasi-periodic subwavelength gratings. The first element is a spiral phase element and the second element is a spherical phase element. We provide a theoretical analysis and an experimental demonstration of the formation of the multiple vortices that comprise scalar vortices and a vectorial vortex. © 2006 Optical Society of America

OCIS codes: 050.2770, 260.5430, 230.5440.

Optical vortices are useful for trapping and rotating microscale and nanoscale particles.[1,2] A considerable amount of attention has been directed to the formation of several vortices by a single beam.[3,4] Several methods have been suggested for this purpose, including the use of liquid crystal devices[3] and computer-generated holograms.[4] However, all these methods are somewhat cumbersome, have low efficiency, or lack the ability to form polarization-dependent vortices.

In this Letter we theoretically analyze and experimentally demonstrate the formation of on-axis polarization-dependent multiple vortices with different topological charges, comprising scalar vortices and a vectorial vortex. A vectorial vortex is formally defined in Ref. 5. Our method is based on combining two geometric phase elements: a spiral phase element and a spherical phase element. This method extends the multiple vortex formation to the third dimension, making it suitable for trapping three-dimensional structures. We used space-variant subwavelength dielectric gratings for the formation of such elements. These quasi-periodic structures perform space-variant polarization manipulation, which inevitably results in spatial geometric phase modulation. The geometric phase was initially investigated by Pancharatnam and Berry, and therefore these elements are aptly referred to as Pancharatnam–Berry phase optical elements (PBOEs).[5–8] We have designed and realized both spiral and spherical phase PBOEs for 10.6 μm wavelength illumination. These elements were etched on a GaAs wafer with a subwavelength period of 2 μm.

The proposed combined element is passive, lightweight, polarization dependent, and highly efficient. The PBOE is realized by a single-mask photolithographic technique that forms a thin aberration-free element that permits the flexible generation of any desired phase front. The use of photolithographic techniques permits the integration of the element onto a chip, which would allow it to be used in diverse applications, including those of a biological nature.

Our concept for the manipulation of polarization-dependent multivortices is presented in Fig. 1(a). A beam of linear polarization is incident upon a spiral phase PBOE followed by a spherical phase PBOE and a refractive lens of focal length f_r. The first PBOE generates a vectorial vortex,[7] which is transmitted through the spherical phase PBOE. The beam is split into three polarization orders. The first order maintains the polarization state of the incident vectorial vortex and converges at $z=f_r$. The second and third orders are right- and left-handed circularly polarized (RCP and LCP) scalar vortices with conjugate topological charges that converge at $z=f_R$ and $z=f_L$, respectively; f_R and f_L are the focal lengths resulting from the combined action of the spherical phase PBOE and the refractive lens for LCP and RCP illumination, respectively.

The analysis of fully polarized monochromatic coherent beams is conveniently performed by the use of the Jones calculus. Recently, we have shown that a PBOE behaves as a space-variant wave plate element with a constant retardation and a space-varying fast axis, $\theta(\boldsymbol{\rho})$, along the transverse plane co-

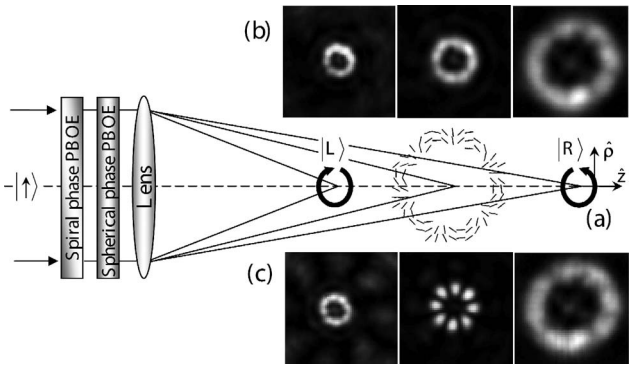

Fig. 1. (a) Concept of the manipulation of a polarization-dependent multivortex beam with quasi-periodic subwavelength gratings. The rounded arrows in the near and far focal planes describe the LCP and RCP states of the focused beams, whereas the inset at the central focal plane depicts the measured orientation angles of the space-variant polarization ellipses. (b) Measured intensity distributions in the three focal planes. (c) Measured intensity distributions in the three focal planes transmitted through a polarizer oriented at 0°.

0146-9592/06/111594-3/$15.00

ordinate, $\boldsymbol{\rho}$.[6–8] The transmission Jones matrix of such an element is given in the helical basis by[8]

$$\mathbf{T} = \frac{t_x + t_y e^{i\phi}}{2}\begin{bmatrix} 1 & 0 \\ 0 & 1 \end{bmatrix} + \frac{t_x - t_y e^{i\phi}}{2}\begin{bmatrix} 0 & e^{i2\theta(\boldsymbol{\rho})} \\ e^{-i2\theta(\boldsymbol{\rho})} & 0 \end{bmatrix}, \tag{1}$$

where t_x and t_y are the transmission coefficients for field components that are polarized parallel and perpendicular to the subwavelength grooves, respectively, and ϕ is the retardation of the subwavelength grating. The transmission matrix of a system composed of several PBOEs is determined by multiplying the matrices of the individual elements composing it. The transmission matrix of our specific device equals $\mathbf{T}_{\mathrm{rl}} \cdot \mathbf{T}_{\mathrm{sp}} \cdot \mathbf{T}_s$, where $\mathbf{T}_s$ is the spiral phase PBOE transmission matrix with an orientation function of $\theta = l\omega/2$. l is an integer and ω is the azimuthal coordinate of the polar coordinate system.[7] $\mathbf{T}_{\mathrm{sp}}$ is the spherical phase PBOE transmission matrix with an orientation function of $\theta = \pi(\sqrt{|\boldsymbol{\rho}|^2 + f^2})/\lambda$, where λ is the incident wavelength and f is the focal length of the spherical phase PBOE when illuminated with RCP light.[6] For both elements we assume $t_x = t_y = 1$ with retardations of $\phi = \pi$ for the spiral phase element and $\phi = \pi/2$ for the spherical phase element. $\mathbf{T}_{\mathrm{rl}}$ is the transmission matrix of the refractive lens.

The Jones vector of the beam emerging from such a configuration, illuminated with arbitrarily polarized light, $|\mathbf{E}_{\mathrm{in}}\rangle$, in a paraxial approximation yields

$$\begin{aligned} |\mathbf{E}_{\mathrm{out}}\rangle = \mathbf{T}_{\mathrm{rl}} \cdot \mathbf{T}_{\mathrm{sp}} \cdot \mathbf{T}_s |\mathbf{E}_{\mathrm{in}}\rangle = \frac{1}{\sqrt{2}}\Bigg[& \exp\left(-\frac{i\pi|\boldsymbol{\rho}|^2}{\lambda f_r}\right)|\mathbf{E}_{\mathrm{l}}\rangle \\ & + \langle \mathbf{R}|\mathbf{E}_{\mathrm{in}}\rangle \exp\left(-il\omega - \frac{i\pi|\boldsymbol{\rho}|^2}{\lambda f_R}\right)|\mathbf{R}\rangle \\ & + \langle \mathbf{L}|\mathbf{E}_{\mathrm{in}}\rangle \exp\left(il\omega - \frac{i\pi|\boldsymbol{\rho}|^2}{\lambda f_L}\right)|\mathbf{L}\rangle\Bigg], \end{aligned} \tag{2}$$

where $|\mathbf{R}\rangle = (1\ 0)^T$ and $|\mathbf{L}\rangle = (0\ 1)^T$ are the Jones vectors for the RCP and LCP states, $|\mathbf{E}_{\mathrm{l}}\rangle = \mathbf{T}_s|\mathbf{E}_{\mathrm{in}}\rangle$, and $\langle \boldsymbol{\alpha}|\boldsymbol{\beta}\rangle$ denotes the inner product of vectors $|\boldsymbol{\alpha}\rangle$ and $|\boldsymbol{\beta}\rangle$. From Eq. (2) it is evident that the emerging beam comprises three polarization orders. In the case of linearly polarized illumination, $|\uparrow\rangle$, the first polarization order is a linearly polarized axially symmetric (LPAS) vectorial vortex with $|\mathbf{E}_{\mathrm{l}}\rangle = [\exp(il\omega)|\mathbf{R}\rangle + \exp(-il\omega)|\mathbf{L}\rangle]/\sqrt{2}$, which is focused at a distance f_r. The second and the third polarization orders are RCP and LCP beams with helical phases of $-l$ and l topological charge converging at the distances $f_R = f_r f/(f - f_r)$ and $f_L = f_r f/(f + f_r)$, respectively. These phase modifications result from the space-variant polarization state manipulation formed by the PBOEs; therefore they are geometric in nature.[6–8] As is evident from Eq. (2), the efficiencies of the polarization orders depend on the incident beam's polarization state and on the PBOE's transmission parameters.[8] Another important feature of the resulting beam is its angular momentum. The RCP and the LCP polarization order beams possess orbital angular momentums of $-\hbar l$ and $\hbar l$ per photon and spin angular momentums of $\hbar$ and $-\hbar$ per photon, respectively.[2–4] However, the first polarization order possesses no angular momentum.[8]

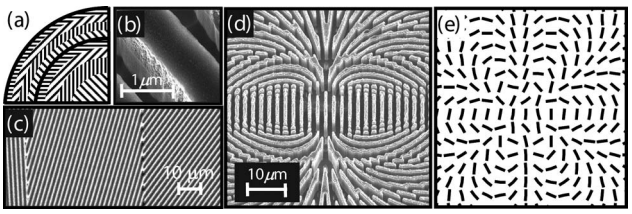

Fig. 2. (a) Magnified geometry of a region on the spherical phase PBOE mask with $N = 4$. (b) and (c) SEM images taken from a small region of the spherical phase PBOE. (d) SEM image of the central part of the spiral phase PBOE. (e) Measured local azimuthal angles of the beam emerging from the spiral phase PBOE.

We implemented the proposed combination of elements by using quasi-periodic subwavelength dielectric gratings. In our approach, the desired continuous phase function $2\theta(\boldsymbol{\rho})$ is approximated by discrete steps of $2\pi/N$, where N is the number of discrete levels.[8] For 2, 4, 8, and 16 discrete phase levels, the diffraction efficiency to the first diffraction order, which is an exact replica of the desired phase, will be 40.5%, 81.1%, 95.0%, and 98.7%, respectively.[7] We realized a binary chrome mask by using high-resolution laser lithography. The mask was 10 mm in diameter with the number of discrete levels $N = 16$ for the spiral phase PBOE and $N = 8$ for the spherical phase PBOE. A subwavelength period of $\Lambda = 2\ \mu$m was selected together with a fill factor $q = 0.5$, on a GaAs wafer, for use with CO_2 laser radiation of 10.6 μm wavelength. Figure 2(a) shows the magnified geometry of a region on a spherical phase PBOE mask with $N = 4$. The realization of a PBOE by using a designed mask is elaborated in Ref. 7. Figure 2(b) shows a scanning electron microscope (SEM) image of a small region on the spherical phase PBOE with a focal length of $f = 200$ mm. Figure 2(c) shows a SEM image of three levels of the realized spherical phase PBOE, and Fig. 2(d) shows a SEM image of a small region on the realized spiral phase PBOE with $l = 4$. The measured birefringent values of the PBOEs were $t_x = 0.85$, $t_y = 0.75$, and $\phi = 0.56\pi$ for the spherical phase PBOE and $t_x = 0.86$, $t_y = 0.74$, and $\phi = 0.97\pi$ for the spiral phase PBOE. These values are close to the theoretical prediction achieved by using rigorous coupled wave analysis.

Following the fabrication, we investigated the spherical phase PBOE by using the setup depicted in Fig. 1, but with a rotating quarter-wave plate (QWP) instead of the spiral phase PBOE. The focal length of the refractive lens was $f_r = 127$ mm. We illuminated the device with a linearly polarized CO_2 laser beam of 10.6 μm wavelength. The rotating QWP was used as a polarization state generator. The three focal planes were placed at f_r, $f_L = 78$ mm, and $f_R = 348$ mm for the first, second, and third polarization orders, respectively. The focal intensities were captured by a Spiricon Pyrocam III camera. Figure 3 depicts the normalized intensity of the three focal spots as a

function of the QWP orientation. As can be seen, the first polarization order does not depend on the polarization state of the illumination, as noted from Eq. (2) for $l=0$. The other two spots depend on the incident polarization state. This figure demonstrates the ability of our device to serve as a bifocal or trifocal polarization-dependent lens.

To form the multiple vortex beam, we used the setup depicted in Fig. 1(a). First, we measured the polarization state of the vectorial vortex emerging from the spiral phase PBOE by using the four-measurement technique.[9] The measured azimuthal angle, shown in Fig. 2(e), rotates about the center, indicating a LPAS vectorial vortex.[5] Next, we measured the intensity distributions of the beams emerging from the combined lens system at the three focal planes [Fig. 1(b)]. As can be seen, the three intensity distributions demonstrate annular shaped beams as expected from vortices. Finally, the polarization states of the three focal spots were measured. One of the measurements, which was obtained by inserting a polarizer oriented at 0°, is presented in Fig. 1(c). The polarization state of the RCP and the LCP orders, as measured in the relevant focal plane, resulted in 98% RCP and 97% LCP with a standard deviation of 1.9% and 5.5%, respectively. Comparing Fig. 1(b) with Fig. 1(c), we see that the intensity distribution of the central focal plane, which corresponds to the first polarization order, was changed from a ringlike shape to a flowerlike shape. This result suggests that the central spot is a LPAS beam and thus is a vectorial vortex.[5] The inset in Fig. 1(a), positioned in the central focal plane, depicts the measured orientation angle of the space-variant polarization state of the vectorial vortex. It is evident that the measured space-variant azimuthal angle is similar to the one depicted in Fig. 2(e). This result indicates that the incident vectorial vortex maintains its polarization state upon propagation. The measured average deviation from the desired polarization orientation was 5% with a standard deviation of 6.2%, indicating good agreement with the theoretical prediction. The small deviations result from the fact that all the focal plane spots contain high intensities from the relevant polarization order and low intensity from the other polarization orders.

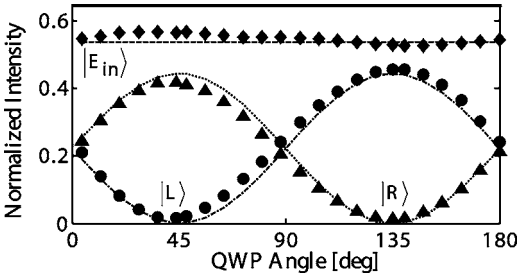

Fig. 3. Normalized intensity at different focuses of the spherical phase PBOE followed by the refractive lens as a function of the orientation of the QWP used as a polarization state generator. Triangles are the measurements in the RCP focal plane, circles are the measurements in the LCP focal plane, and diamonds are the measurements in the focal plane of the first polarization order. The dotted, dashed–dotted, and dashed curves are the theoretical calculations for each order.

To conclude, we demonstrated the formation of multiple vortices having different topological charges comprising scalar vortices and a vectorial vortex when a spherical phase PBOE was illuminated with a vectorial vortex beam. The formation of the incident vectorial vortex was achieved by illuminating a spiral phase PBOE with linearly polarized light. Both PBOEs were realized by using quasi-periodic subwavelength gratings. In the case of circularly polarized illumination, the combined PBOEs together with the refractive lens produce only two scalar vortices with orthogonal circular polarization. No vectorial vortex is observed; this result can be calculated by using Eq. (2). Another interesting case is unpolarized illumination in which the emerging beam contains three polarization orders. The second and third polarization orders are scalar vortices with conjugate helical phases and orthogonal circularly polarized states that are focused in the near and far focal planes, as achieved by a linearly polarized illumination. These polarization orders possess orbital angular momentum and spin angular momentum as stated above. However, the first polarization order is an annular beam with zero angular momentum and zero degree of polarization focused at the central focal plane. The formalism used for calculating this case can be found in Ref. 10.

E. Hasman's e-mail address is mehasman @tx.technion.ac.il.

References

1. K. T. Gahagan and G. A. Swartzlander, Jr., Opt. Lett. **21**, 827 (1996).
2. N. B. Simpson, K. Dholakia, L. Allen, and M. J. Padgett, Opt. Lett. **22**, 52 (1997).
3. K. Ladavac and D. G. Grier, Opt. Express **12**, 1144 (2004).
4. J. Leach, M. R. Dennis, J. Courtial, and M. J. Padgett, Nature **432**, 165 (2004).
5. A. Niv, G. Biener, V. Kleiner, and E. Hasman, Opt. Lett. **30**, 2933 (2005).
6. E. Hasman, V. Kleiner, G. Biener, and A. Niv, Appl. Phys. Lett. **82**, 328 (2003).
7. A. Niv, G. Biener, V. Kleiner, and E. Hasman, Opt. Commun. **251**, 306 (2005).
8. E. Hasman, G. Biener, A. Niv, and V. Kleiner, in *Progress in Optics, Vol. 47*, E. Wolf, ed. (Elsevier, 2005), p. 215.
9. C. Brosseau, *Fundamentals of Polarized Light; A Statistical Optics Approach* (Wiley, 1998).
10. Y. Gorodetski, G. Biener, A. Niv, V. Kleiner, and E. Hasman, Opt. Lett. **30**, 2245 (2005).